Biophysical Chemistry, 32 (1988) 121–130
Elsevier

BPC 01318

Pressure dependence of fluorescence quenching reactions in proteins

Maurice R. Eftink [a] and Zygmunt Wasylewski [b]

[a] *Department of Chemistry, University of Mississippi, University, MS 38655, U.S.A.*
and [b] *Department of Biochemistry, Jagiellonian University, Krakow, Poland*

Received 10 March 1988
Accepted 1 August 1988

Fluorescence quenching; Pressure dependence; Activation volume; Volume change; Melittin; Parvalbumin; Ribonuclease T_1; *N*-Acetyl-L-tryptophanamide; Fluorescence lifetime

The effect of hydrostatic pressure (0–2.6 kbar) on the acrylamide quenching of the fluorescence of indole derivatives and several single-tryptophan-containing proteins has been studied using phase fluorometry at 25 °C. For the model system, *N*-acetyl-L-tryptophanamide in water, there is essentially no pressure dependence of the quenching rate constant, k_q. For the internal Trp residue of ribonuclease T_1 and cod parvalbumin, there also is essentially no pressure dependence of the apparent k_q at low pressure. Thus, the activation volume, $\Delta V^{\ddagger}$, for these quenching processes is approximately zero. Such small $\Delta V^{\ddagger}$ values are expected for diffusion-limited reactions in water at this temperature. The low, apparent $\Delta V^{\ddagger}$ values for the globular proteins characterize these quenching processes as involving very small amplitude fluctuations in the protein structures. Only for the poised tetramer $\rightleftharpoons$ monomer equilibrium of melittin were we able to observe a significant effect of pressure on k_q and this is due to the pressure-induced shift in the equilibrium position.

1. Introduction

Hydrostatic pressure can be a very useful intensive parameter for perturbing chemical reactions [1–4]. There have been a number of studies of the influence of pressure, P, on the thermodynamics of protein-ligand interactions and structural transitions in proteins [1,2,5]. In general, increased P tends to cause oligomeric proteins to dissociate and globular proteins to 'denature'. The latter effect usually occurs at several thousand bar. For pressures below that for 'denaturation', one would expect some perturbation of the dynamic properties of proteins. However, there have been very few studies that may sense the effect of P on the conformational dynamics of proteins [6–8]. Two previous studies are the effect of P on the hydrogen isotope exchange kinetics of proteins [6] and the P dependence of the flipping of aromatic rings (NMR relaxation) in bovine trypsin inhibitor [7].

Fluorescence solute quenching reactions are a type of reaction that is amenable to P studies, since the reaction is initiated by light and can be monitored within a pressure cell with quartz windows [3]. Only a few studies of the P dependence of fluorescence quenching reactions have been reported [9,10]. Quenching studies with proteins have proved to be very valuable in assessing the degree of solvent exposure of Trp residues and, in cases where the fluorescent Trp residue is located in the interior of proteins, the rate of solute quenching reactions can be related to the conformational dynamics of proteins [11–14].

Here we report studies of the P dependence of the quenching of the intrinsic tryptophanyl (Trp) fluorescence of globular proteins using the polar quencher, acrylamide [11,12]. The proteins that we have studied include ribonuclease T_1 and cod parvalbumin, which possess single, internal Trp

Correspondence address: M.R. Eftink, Department of Chemistry, University of Mississippi, University, MS 38655, U.S.A.

residues [13,15]. We have monitored the fluorescence quenching via lifetime measurements using the phase/modulation method [16]. By measuring fluorescence lifetimes, instead of steady-state intensities, we avoid complications due to static quenching and any artifactual changes in the fluorescence signal due to *P*-induced changes in the optical transmission of the pressure cell or problems in repositioning the pressure cell after the addition of quencher to the sample.

2. Experimental

2.1. Materials

Ribonuclease T_1 from *Aspergillus oryzae* was a gift from Dr. Frederick Walz, Jr, Kent State University. Cod parvalbumin was purified as described elsewhere [13]. Monellin from *Dioscorephyllum cumminsii,* bee venom melittin and *N*-acetyl-L-tryptophanamide (NATA) were obtained from Sigma. Acrylamide was recrystallized from ethyl acetate.

2.2. Methods

Fluorescence lifetime measurements were made with two different instruments. In our laboratory, an SLM 4800 phase/modulation fluorometer, equipped with a Pockels cell modulator from ISS, was used. Samples were excited through an interference filter centered at 290 nm, and emission was observed through a bandpass filter. A modulation frequency of 30 MHz was employed. *p*-Terphenyl was used as a reference. Since a high-pressure chamber was used, the reference measurements were made before and at the end of the experimental measurements. We find that the reference phase angle is very stable, for a period of hours, with the Pockels cell modulator. The second instrument for measuring lifetimes was the Nd-YAG based phase/modulation fluorometer at the Fluorescence Dynamics Laboratory at the University of Illinois. This system uses the harmonic overtones of the mode-locked laser as the means of modulating the light beam. The system includes a dye laser and a frequency doubler, which enabled selection of an excitation beam at 295 nm. Emission was observed at the λ_{max} of the sample, using a monochromator. With this system we used the scatter from the sample as the reference. For the NATA and protein solutions, a small amount of glycogen was added to produce a scattered light signal (at 290 nm) that was about equal to the fluorescence signal. By using scattered light, alternate measurements of signal and reference were possible. For most measurements, a modulation frequency of 57.2 MHz was used.

Increased pressure was achieved by use of a high-pressure cell, designed by Paladini and Weber [17]. Dr. William Mantulin, University of Illinois, kindly allowed us the use of his high-pressure cell. Pressure was generated by a piston screw pump from High Pressure Equipment (Erie, PA). Fluorescence lifetime measurements were made at pressure intervals between 0 and 2600 bar. The lifetimes were found to be reversible, upon increasing and then decreasing pressure. In instances in which this reversibility was not obtained, the data were discarded.

Multifrequency phase/modulation data were fitted to monoexponential, biexponential or continuous-distribution models with the nonlinear least-squares program of Beechem and Gratton [18]. This program was also used to perform a simultaneous (global) analysis of data at several pressures.

3. Results

3.1. Model systems

The effect of hydrostatic pressure on the fluorescence lifetime (average of phase and modulation lifetimes) of NATA, in the absence and presence of the quencher, acrylamide, is shown in fig. 1A. The τ value decreases with increasing P in this experiment. In other experiments with indole, 3-methylindole and NATA, and with a different phase fluorometer, we have seen both slight increases and decreases in τ with P. Apparently the absolute variation in τ with P depends upon some subtle characteristics of the fluorometer, the pressure cell, the sample bottle or its exact position in

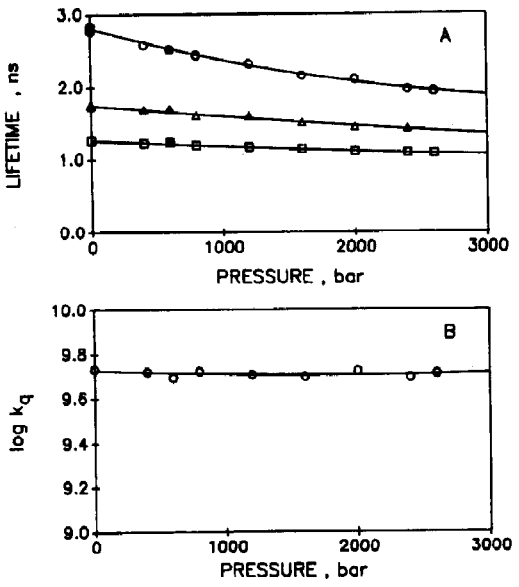

Fig. 1. (A) Pressure dependence of the fluorescence lifetime of NATA in water, in the absence (○) and presence of 40 mM (△) and 80 mM (□) acrylamide. Closed symbols are measurements made upon releasing pressure. (B) Plot of log k_q vs. P.

the light beam, and we have not been able to identify the cause of the differences. Nevertheless, with each phase fluorometer we were able to obtain reproducible patterns. Thus, we can compare the P dependence of a sample, in the absence and presence of quencher, to determine the P dependence of the apparent quenching rate constant, k_q. The value of k_q is calculated via eq. 1, where τ_0 and τ are the respective lifetimes in the absence and presence of quencher, Q.

$$k_{q(app)} = \left(\frac{\tau_0}{\tau} - 1\right)/[Q]\tau_0 \qquad (1)$$

The P dependence of the quenching by acrylamide of the fluorescence of NATA and indole, in water at 25 °C, is shown in fig. 1B. Essentially no P dependence is observed in either case.

The P dependence of k_q can be interpreted in terms of an activation volume, $\Delta V^{\ddagger}$, for the reaction, as given by the following expression [3,4]

$$\log k_{q(app)} = A - \frac{\Delta V^{\ddagger} P}{2.303RT} \qquad (2)$$

where A is a pre-exponential factor (i.e., related to the rate constant at near-zero pressure), and R the gas constant (82.05 atm/mol per K). From the plots in fig. 1B, $\Delta V^{\ddagger}$ values of about 0.05 ± 0.05 ml/mol are found for the collisional quenching of indole (or NATA) by acrylamide in water.

This $\Delta V^{\ddagger}$ may seem surprisingly small for a bimolecular reaction [3]. However, the quenching is a diffusion-controlled reaction [12] and is limited only by diffusion through the bulk solvent. Whereas the viscosity, η, of most solvents increases with P, the η of water is known to be almost independent of P near 30 °C [19,20]. In fig. 2 is shown the dependence of $\log(1/\eta)$ on P. The viscosity of water increases by only 4% as P increases from 0.001 to 2600 bar at 30 °C. Thus, a 4% reduction in $k_{q(app)}$ would be expected from this effect.

Compression of the solvent will also have a small effect on the $k_{q(app)}$. As P increases to 2600 bar there will be a 8% decrease in the volume of the aqueous sample [21]. This, in turn, will increase the concentration of the quencher by 8%, which should result in an increase in $k_{q(app)}$ (if the [Q] is not adjusted for the compression effect). Thus, the two effects of P (i.e., viscosity increase and compression of water) are both small and in opposite directions. The effects partially cancel and should give rise to only about a 4% increase in $k_{q(app)}$ as P increases to 2600 bar (i.e., these effects can account for a $\Delta V^{\ddagger}$ of about -0.01 ml/mol). In other words, these effects will not produce a noticeable $\Delta V^{\ddagger}$ and the near-zero $\Delta V^{\ddagger}$ that we observe for the acrylamide quenching of indole (or NATA) must mean that there truly is a

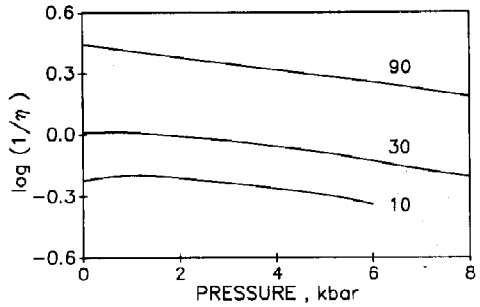

Fig. 2. Pressure dependence of the viscosity of water at 10, 30 and 90 °C. Taken from the data of Wilbur et al. [19].

negligible activation volume for the quenching reaction.

3.2. Single-tryptophan-containing proteins

Next we studied the P dependence of the acrylamide quenching of the single tryptophan residues in the proteins ribonuclease T_1, cod parvalbumin and monellin. The Trp residues in the first two are known to be buried inside these small globular proteins [13,15]. The Trp of monellin lies on the surface of this protein [22]. The fluorescence decay of each protein is non-exponential at the pH studied (for ribonuclease T_1 it is a single exponential at pH 5, but not at pH 7) [15]. However, the departure from a single-exponential decay is not large for each of these and the fluorescence lifetime values given below are the average of the phase and modulation lifetimes (at 30 or 57.8 MHz). Such an averaged τ is approximately equal to the weighted average lifetime for a multiexponential decay, which is appropriate for calculating a $k_{q(app)}$ via eq. 1.

Shown in fig. 3A is the pressure dependence of the fluorescence lifetime of ribonuclease T_1 in the absence and presence of two concentrations of acrylamide. The lifetimes are found to vary little with P. In fig. 3B are shown plots of log $k_{q(app)}$ vs. P for ribonuclease T_1, parvalbumin and monellin. As with the model systems above, there is no significant variation of $k_{q(app)}$ with P. Activation volumes of 0.56 ± 0.15, -0.10 ± 0.2 and -0.5 ± 0.1 ml/mol for ribonuclease T_1, parvalbumin and monellin, respectively, are calculated from the initial slopes of these plots. A slight upward trend is seen for the data for monellin above 2000 bar.

The very low $\Delta V^{\ddagger}$ values must be characteristic of the rate-limiting step for the collision between acrylamide and the Trp residues of these proteins. For the surface Trp of monellin, presumably the rate-limiting step is diffusion of acrylamide through the bulk, and, in view of the small $\Delta V^{\ddagger}$ found for the model systems, it is reasonable that the $\Delta V^{\ddagger}$ for monellin is also small.

For the internal Trp residues in ribonuclease T_1 and parvalbumin, two kinetic models have been considered in the past for the solute quenching

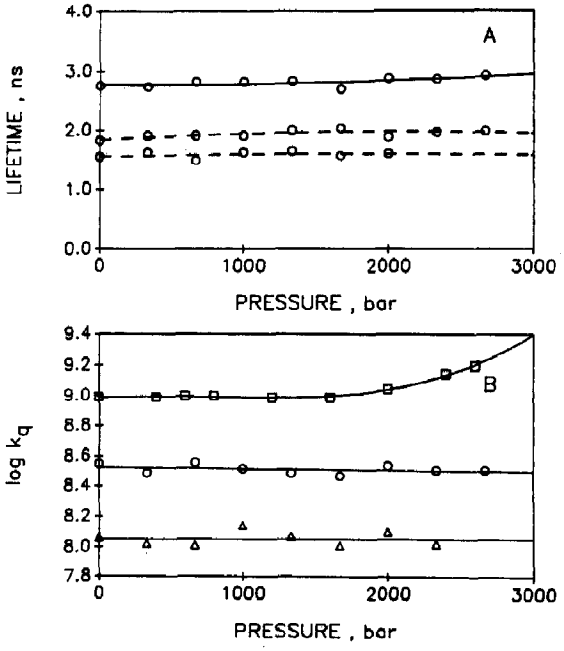

Fig. 3. (A) Pressure dependence of the fluorescence lifetime of ribonuclease T_1 in the absence (top) and presence of 500 mM (middle) and 780 mM (bottom) acrylamide. (B) Plots of log k_q vs. P for monellin (□), ribonuclease T_1 (○), and parvalbumin (△).

reaction. These are the penetration model [23,25] and the unfolding model [24]. For the penetration model, the apparent k_q will be limited by the stepwise diffusion of the quencher into the matrix of the globular protein. This penetration process is expected to be facilitated by rapid, small-amplitude fluctuations in the structure of the protein [11,14,23,25]. For the unfolding model, the apparent k_q will be equal to $k_d K_{un}$, where k_d is the rate constant for diffusion of the quencher through the bulk solution and K_{un} an equilibrium constant for the segmental unfolding of a part of the protein to expose the Trp residue to the bulk [24,25].

For the unfolding mechanism one would expect a contribution to the apparent $\Delta V^{\ddagger}$ from the protein unfolding transition. The unfolding (denaturation) of a globular protein is usually characterized by a volume change, $\Delta V^{\ddagger}$ of -30 to -100 ml/mol [1,2], depending on the size of the protein. This roughly corresponds to a decrease of

about 1% in the total molar volume of a globular protein as it unfolds. This negative ΔV^0 is thought to be due to the existence of packing voids in the folded state and to the solvation of apolar side chains (upon unfolding). Thus, a $\Delta V^{\ddagger}$ of similar magnitude would be expected if the solute quenching of an internal Trp residue occurs by an unfolding mechanism. The observed values $\Delta V^{\ddagger} \approx 0$ are not consistent with such a mechanism, or at least the result requires the unfolding transition to be very limited in extent.

The near-zero $\Delta V^{\ddagger}$ for parvalbumin and ribonuclease T_1 are consistent with a penetration model, in which the small-amplitude conformational fluctuations occur with little change in the total volume of the system. If 'holes' are transiently created in one region of the protein to facilitate quencher penetration, then other regions (of the protein or surrounding solvent) must become more densely packed. The 'mobile defect' hypothesis of Lumry and Rosenberg [26] is an appropriate model for understanding our results. Other recent studies also support the penetration model for the interpretation of solute quenching data [25,27].

3.3. Melittin tetramer ⇌ monomer equilibrium

The results presented to this point show no significant P dependence for the acrylamide quenching of the fluorescence of either model aqueous systems or globular proteins. To demonstrate that a P dependence (and non-zero $\Delta V^{\ddagger}$) can be observed when one exists, we performed the following studies with bee venom melittin and its monomeric and tetrameric forms.

At low ionic strength and neutral pH, melittin (2.8 kDa) is a monomer, M, with a random coil structure. At high ionic strength (i.e., 2 M NaCl), melittin exists as a tetramer, T. The T ⇌ M equilibrium can be shifted by varying ionic strength, within this range, or by varying the melittin concentration or pH [28,29]. Thompson and Lakowicz [30] also demonstrated, using fluorescence anisotropy measurements, that the T ⇌ M equilibrium can be shifted to the monomeric form by increased hydrostatic pressure. They analyzed their data to obtain $\Delta V^0 = -150$ ml/mol for the dissociation of the tetramer to four monomers. (This

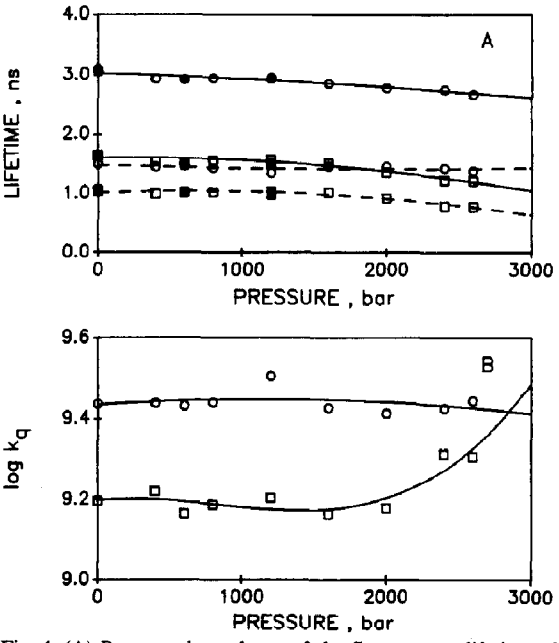

Fig. 4. (A) Pressure dependence of the fluorescence lifetime of melittin monomer (○) and tetramer (□). (———) In the absence of quencher; (- - - - -) in the presence of 127 and 221 mM quencher, for monomer and tetramer, respectively. (B) Plots of log k_q vs. P for melittin monomer (○) and tetramer (□).

negative ΔV^0 was observed at low P; at higher P the apparent ΔV^0 was found to become more positive.)

The accessibility of the single Trp residue of melittin to the quencher acrylamide is larger for the monomeric state ($K_{sv} \approx 9$ M^{-1}) than for the tetrameric state ($K_{sv} \approx 3.5$ M^{-1}) [27]. Thus, this T ⇌ M equilibrium of melittin was selected to demonstrate a P-induced change in the apparent rate constant for acrylamide quenching. If, for example, we start with a poised T ⇌ M equilibrium (which, we will call a mixture), achieved by using an NaCl concentration of 0.5 M [30], and then increase P, we should shift the equilibrium toward the monomeric state and should observe an increase in the apparent acrylamide k_q.

First we measured the P dependence of the fluorescence lifetime of the monomeric (0.01 M Tris-HCl, pH 8) and tetrameric (2.0 M NaCl, pH 8) forms of melittin, as shown in fig. 4A. This was done in the absence and presence of acrylamide,

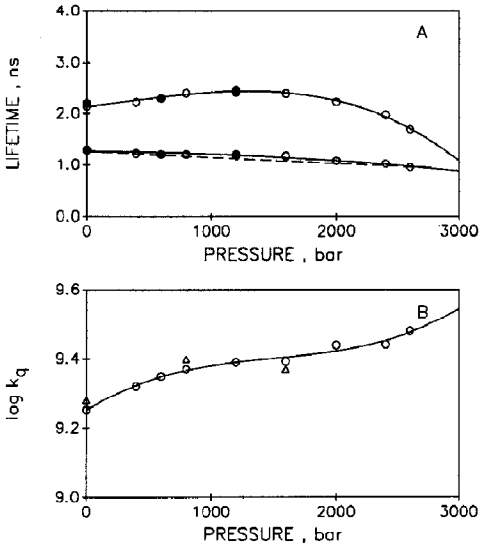

Fig. 5. (A) Pressure dependence of the fluorescence lifetime of a mixture of melittin monomer and tetramer (0.5 NaCl, pH 8.0). (———) In the absence of quencher; (- - - - - -) in the presence of 173 mM acrylamide. (B) Plot of log k_q vs. P. The initial slope gives $\Delta V^{\ddagger} = -15$ ml/mol.

in order to allow determination of the apparent k_q for each state as a function of P. In fig. 4A we report average $(\tau_p + \tau_m)/2$ values determined at 57.2 MHz. The decay of both the M and T states is nonexponential and a more correct approach is to obtain and analyze multifrequency phase and modulation data. This more complete analysis will be presented below. In fig. 4B are shown plots of log k_q vs. P for the M and T states the melittin. As with other proteins, we find essentially no (initial) P dependence for the solute quenching of the M and T forms. A slight increase in log k_q data for the T form is seen at high P. We do not have sufficient data at this time to decide whether this is a real effect (i.e., P-induced dissociation of the tetramer, even at high salt) or if it is just experimental error.

Subsequently, we performed a similar P dependence study with a solution of melittin which was poised at the T ⇌ M equilibrium (0.5 M, 100 μM melittin, 0.01 M Tris-HCl, pH 8). As shown in fig. 5A, at ambient P the average $((\tau_p + \tau_m)/2)$ lifetime, obtained at 57.2 MHz, is midway between the average τ for the M and T forms. As P is increased, the average τ of the mixture increases and approaches the average τ for the M form P between 1000 and 2000 bar. From the average τ obtained in the presence of acrylamide we determined the apparent k_q as a function of P (see fig. 5B). At ambient P, the apparent k_q is midway between that for the M and T states. As P is increased, the apparent k_q increases and approaches that of the M state. From the initial slope of the plot of log k_q vs. P, a $\Delta V^{\ddagger}$ of about -15 to -20 ml/mol is obtained at low P.

Thus, our P dependence acrylamide quenching studies can report a non-zero $\Delta V^{\ddagger}$, when one exists, and this makes believable our near-zero $\Delta V^{\ddagger}$ reported above for simple globular proteins.

A couple of concerns regarding these studies with melittin are that (i) the fluorescence decays of both the M and T states of melittin are nonexponential and single-frequency, average τ values may introduce some error, and (ii) the observed, initial $\Delta V^{\ddagger}$ is a complex value and is only partially weighted toward the ΔV^0 for the T ⇌ M transition, and, in principle, it should be possible to extract the ΔV^0 for the T ⇌ M transition from the data in fig. 5. We will address the first matter here and the second matter in section 3.4.

We have collected multifrequency phase and modulation data for the M and T states of melittin. These data can be fitted by a double-exponential decay. In table 1 we list best-fit values for τ_i and α_i for the M and T states. For a mixture of states in 0.5 M NaCl, as many as seven fitting

Table 1

Discrete lifetime fits for multifrequency phase/modulation data for melittin

Conditions for monomer; 0.01 M Tris-HCl buffer, pH 8.0; for tetramer, 2.0 M NaCl, 0.01 M Tris-HCl, pH 8.0; for mixture, 0.5 NaCl, 0.01 M Tris-HCl, pH 8.0; 25°C in all cases. All lifetimes in ns. Errors of ±0.5 and ±0.005 were used for the phase and modulation measurements in the calculation of χ^2 values.

	τ_1	τ_2	α_1	χ^2
Monomer ($P = 1$ bar)	1.64	3.96	0.501	2.8
Tetramer ($P = 1$ bar)	0.99	2.79	0.834	5.1
Mixture ($P = 1$ bar)	1.20	3.53	0.725	3.4

Table 2

Lorentzian distribution fits to multifrequency phase/modulation data for melittin

See table 1 for conditions. Central lifetimes, $\bar{\tau}_i$ and width, Δ_i, are in ns.

	$\bar{\tau}_1$	Δ_1	$\bar{\tau}_2$	Δ_2	α_1	χ^2
Monomer, $P=1$ bar	2.54	1.23	–	–	1.0	3.1
Tetramer, $P=1$ bar	–	–	1.05	0.70	0.0	5.2
Mixture, $P=1$ bar	2.89	1.08	1.21	0.48	0.485	3.9
Mixture, biomodal, global fit for						
$P=1$	2.65	1.00	1.15	0.62	0.442	5.2
$P=800$ bar					0.596	
$P=1600$ bar					0.601	
$P=2400$ bar					0.269	
Mixture, unimodal fit						
$Q=0$, $P=1$ bar	1.46	1.16	–	–	1.0	3.0
$P=800$ bar	1.83	1.09	–	–	1.0	2.6
$P=1600$ bar	1.91	1.00	–	–	1.0	3.0
Mixture, unimodal fit						
$Q=0.173$ M, $P=1$ bar	0.99	0.48	–	–	1.0	1.8
$P=800$ bar	1.00	0.37	–	–	1.0	5.3
$P=1600$ bar	1.08	0.19	–	–	1.0	6.2

parameters would be needed to give a double-exponential fit for each state.

Alternatively, we have fitted our lifetime data to a Lorentzian distribution of decay times [31]. As shown in table 2, a good fit is obtained with a distribution centered ($\bar{\tau}$) at 2.54 ns, with a full-width-half-maximum (Δ) of 1.23 ns, for the M state, and $\bar{\tau}=1.05$ ns and $\Delta=0.70$ ns for the T state. Likewise, for mixtures (0.5 M NaCl) the $\bar{\tau}$ from a unimodal distribution fit, in the absence and presence of quencher, can be used to obtain an apparent k_q. This approach is an improvement over the use of only single-frequency lifetime data, but, as shown by the symbol Δ in fig. 5B, it yields approximately the same pattern for the apparent k_q.

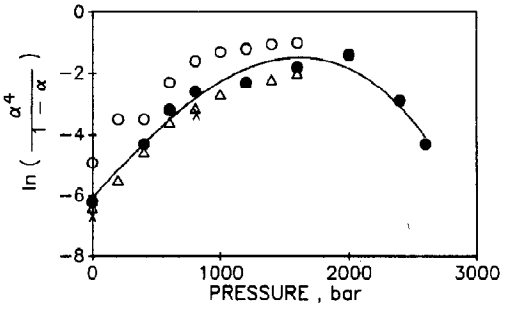

Fig. 6. Pressure dependence of $\ln(\alpha^4/1-\alpha))$ for the melittin T ⇌ M equilibrium. (●) Obtained from initial K_{sv} data; (○, △) taken from anisotropy studies of Thompson and Lakowicz [30]. For the latter points the upper set corresponds to 100 μM melittin and the lower set to 200 μM melittin, both at 0.5 M NaCl. Our values (●, ×) are from studies at 100 μM melittin, 0.5 M NaCl.

3.4. ΔV^0 for $T \rightleftharpoons M$ transition in melittin

Thompson and Lakowicz [30] used the P dependence of the fluorescence anisotropy of melittin to determine the ΔV^0 for the tetramer dissociation. Here we show that the apparent acrylamide k_q can also be used to determine the ΔV^0. First we present a few relationships which describe the tetramer dissociation.

$$T \rightleftharpoons 4M \tag{3}$$

$$\alpha_m = \frac{[M]}{[M]+[T]} = \frac{[M]}{[M]_0} \tag{4}$$

$$K_d = \frac{[M]^4}{[T]} = \frac{4\alpha_m^4[M]_0^3}{(1-\alpha_m)} \tag{5}$$

$$\frac{d \ln K_d}{dP} = \frac{-\Delta V^0}{RT} \tag{6}$$

Here α_m is the fraction of total melittin that is in the monomeric state. If α_m can be obtained, a plot of ln K_d (or ln $\alpha_m^4/(1-\alpha_m)$) vs. P will yield ΔV^0.

Values of α_m can be estimated from the fluorescence quenching results in fig. 5 as follows. Let us assume that the apparent Stern-Volmer quenching constant is approximately equal to

$$K_{sv(app)} \approx f_t K_{sv,t} + f_m K_{sv,m} \tag{7}$$

where $K_{sv,t}$ and $K_{sv,m}$ are the quenching constants for the T and M states (which can be obtained separately), and f_t and f_m the fractions of the total emission that are due to the T and M states, respectively. From known $K_{sv,t}$ and $K_{sv,m}$ values, one can determine f_m as

$$f_m \approx \frac{K_{sv(app)} - K_{sv,t}}{1 - K_{sv,t}/K_{sv,m}} \tag{8}$$

which is related to α_m as follows

$$\alpha_m = 1 + \frac{\Phi_m}{\Phi_t}(f_m - 1) \tag{9}$$

where Φ_m and Φ_t are the relative quantum yields of the M and T states (which we assume to be the same), respectively. From $K_{sv,app}$ values obtained from the data in fig. 5 for the T ⇌ M mixture, we obtained α_m values, which were then plotted as ln $(\alpha_m^4/(1-\alpha_m))$ vs. P in fig. 6 (filled circles).

Also shown in fig. 6, as open symbols, are values obtained by Thompson and Lakowicz [30] using steady-state fluorescence anisotropy measurements, made as a function of P. From the initial slope through our values we find $\Delta V^0 = -150 \pm 30$ ml/mol. This value is in agreement with that reported by Thompson and Lakowicz. We also find that the ΔV^0 becomes more positive as P is increased above 2000 bar. Between 1 and 1600 bar, an increase in P shifts the equilibrium toward the M state, but this shift appears never to become complete. A further increase may induce association, but our data are too limited at this time to prove this point.

The P-induced shift of melittin from the T to M state can also be seen in the multi-frequency phase and modulation data in fig. 7. The left-most and right-most patterns in this figure are data for melittin monomer (○, ●) and tetramer (□, ■), respectively. Fits of these data to double-exponential and Lorentzian distribution decay models are given in tables 1 and 2. Data for the poised T ⇌ M mixture, in 0.5 M salt at 1 bar, are shown as the triangles (△, ▲) in fig. 7. As P is increased to 800 bar, the pattern for the mixture shifts to the left, as shown by the inverted triangles (▽, ▼). That is, the apparent phase and modulation lifetimes increase and approach those of the monomeric state. We have performed a simultaneous nonlinear least-squares fit for data sets obtained for the mixture at 1, 800, 1600 and 2400 bar. The fit was accomplished by using the program GLOBAL, written by Beechem and Gratton [18]. As shown in table 2, this global fit yields $\bar{\tau}_1 = 2.65$ ns, $\Delta_1 = 1.00$ ns, $\bar{\tau}_2 = 1.15$ ns and $\Delta_2 = 0.62$ ns. The α_1 value, which is the fraction of light that is absorbed by the monomeric species of melittin, is found to increase as P is increased from 1 to 1600 bar; as P is increased to 2400 bar, α_1 decreases. Thus, these multifrequency lifetime results are in qualitative agreement with the above acrylamide quenching studies.

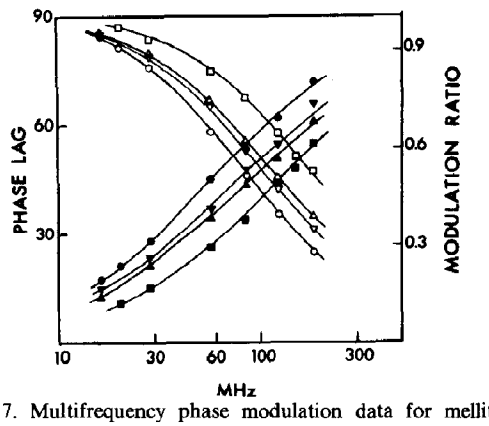

Fig. 7. Multifrequency phase modulation data for mellitin monomer (○, ●), tetramer (■, □) and mixture in 0.5 NaCl at 1 bar (△, ▲) and 800 bar (▽, ▼). Closed symbols, phase angles; open symbols, modulation ratios. The solid lines represent a simultaneous global fit of these data sets, plus two additional data sets for the mixture at 1600 and 2400 bar. The parameters for the global fit are given in table 2.

4. Discussion

Our studies show that the apparent $\Delta V^{\ddagger}$, for acrylamide quenching of the fluorescence of Trp residues in proteins, is approximately zero for several proteins. This is consistent with the action of small-amplitude fluctuations in the structure of a protein (for internal Trp residues) or the solvent (for surface Trp residues) to facilitate the quenching process. Only when a poised two-state transition is perturbed by pressure, such as the melittin $T \rightleftharpoons M$ equilibrium, do we find a significant change in the quenching rate constant with pressure and an apparent negative $\Delta V^{\ddagger}$. Dissociation of melittin can be considered a model for the unfolding mechanism for the quenching of internal Trp residues in proteins. If such a mechanism is utilized, the studies with melittin suggest that a negative $\Delta V^{\ddagger}$ should be observed for the quenching reaction. The near-zero $\Delta V^{\ddagger}$ we find for several proteins favors the penetration mechanism for solute quenching.

It is difficult to offer further interpretation regarding these near-zero $\Delta V^{\ddagger}$. Carter et al. [6] also reported a small $\Delta V^{\ddagger}$ (3 ± 2 ml/mol) associated with the 'protein' component of hydrogen isotope exchange kinetics (i.e., the difference in $\Delta V^{\ddagger}$ between the protein and a polypeptide) with proteins. However, Wüthrich et al. [7] reported a large $\Delta V^{\ddagger}$ of 30 ml/mol for the flipping of aromatic rings in pancreatic trypsin inhibitor and Karplus and McCammon [32] rationalized this $-\Delta V^{\ddagger}$ in terms of the compressibility of the protein. They assumed a compressibility value for the protein equal to that of an apolar organic solvent. Proteins have a heterogeneous structure and experimental (adiabatic) compressibility values for proteins are known to be significantly lower (1/5–1/10) than those for either water or organic solvents [2]. Gekko and Hasegawa [33] have tabulated compressibility values, ranging from -1.11 to 10.9×10^{-12} cm^2/dyn for a large group of proteins. It is believed that oily regions in proteins make the largest (positive) contribution to the total compressibility and that α-helix regions and other relatively stiff, hydrogen-bonded regions contribute much less to the compressibility. So it is difficult to relate a global, thermodynamic property (compressibility) to specific dynamic events and it is possible that there will be different effects of pressure on different events and regions in a protein. Also, Gekko and Noguchi [34] have made the important observation that about 3–6% of the volume of a globular protein exists as cavity space. Movement of these cavities may provide a mechanism for penetration by solutes, such as fluorescence quenchers.

Acknowledgements

We express our appreciation to Dr. William Mantulin, University of Illinois, for loaning us his high-pressure chamber. Some of this work was performed at the Laboratory for Fluorescence Dynamics, at the University of Illinois, and we thank Drs. C. Royer, M. van de Ven and other staff members for their helpful assistance. This research was supported by National Science Foundation Grant DMB 85-11569.

References

1 K. Heremans, Annu. Rev. Biophys. Bioeng. 11 (1982) 1.
2 G. Weber and H.G. Drickamer, Q. Rev. Biophys. 16 (1983) 89.
3 C.A. Eckert, Annu. Rev. Phys. Chem. 23 (1972) 239.
4 E. Morild, Adv. Protein Chem. 34 (1981) 93.
5 A.A. Paladini and G. Weber, Biochemistry 20 (1981) 2587.
6 J.V. Carter, D.G. Knox and A. Rosenberg, J. Biol. Chem. 253 (1978) 1947.
7 K. Wüthrich, G. Wagner, R. Richarz and W. Baum, Biophys. J. 32 (1980) 549.
8 M.C. Marden, G.H.B. Hoa and F. Stetzkowski-Marden, Biophys. J. 49 (1986) 619.
9 G. Weber, F. Tanaka, B.Y. Okamoto and H.G. Drickamer, Proc. Natl. Acad. Sci. U.S.A. 71 (1974) 1264.
10 M. Okamoto and H. Teranishi, J. Phys. Chem. 88 (1984) 5644.
11 M.R. Eftink and C.A. Ghiron, Biochemistry 16 (1977) 5546.
12 M.R. Eftink and C.A. Ghiron, Anal. Biochem. 114 (1981) 199.
13 M.R. Eftink and K.A. Hagaman, Biophys. Chem. 22 (1985) 173.
14 J.R. Lakowicz and G. Weber, Biochemistry 12 (1973) 4171.
15 M.R. Eftink and C.A. Ghiron, Biophys. J. 52 (1987) 467.
16 D.M. Jameson, E. Gratton and R.D. Hall, Appl. Spectrosc. Rev. 20 (1984) 55.

17 A.A. Paladini and G. Weber, Rev. Sci. Instrum. 52 (1981) 419.
18 J.M. Beechem and E. Gratton, Proceeding of SPIE, vol. 909 (1988) in the press.
19 D.J. Wilbur, T. DeFries and J. Jonas, J. Chem. Phys. 65 (1976) 1783.
20 L.A. Woolf, J. Chem. Soc. Faraday Trans. 72 (1976) 1267.
21 D. Eisenberg and W. Kauzmann, The structure and properties of water (Oxford University Press, New York, 1969).
22 C.M. Ogata and S.-H. Kim, Biophys. J. 49 (1986) 438a.
23 E. Gratton, D.M. Jameson, G. Weber and B. Alpert, Biophys. J. 45 (1984) 789.
24 D.B. Calhoun, J.M. Vanderkooi and S.W. Englander, Biochemistry 22 (1983) 1533.
25 M.R. Eftink and K.A. Hagaman, Biophys. Chem. 25 (1986) 277.
26 R. Lumry and A. Rosenberg, in: L'eau: et les systemes biologiques (Centre National de la Recherche Scientifique, Paris, 1975) p. 53.
27 M.R. Eftink and C.A. Ghiron, Biochemistry 23 (1984) 3891.
28 J.C. Talbot, J. Dufourcq, J. de Bony, J.F. Faucon and C. Lussan, FEBS Lett. 102 (1979) 191.
29 J. Bello, H.R. Bellow and E. Granados, Biochemistry 21 (1982) 461.
30 R.B. Thompson and J.R. Lakowicz, Biochemistry 23 (1984) 3411.
31 J.R. Alcala, E. Gratton and F.G. Prendergast, Biophys. J. 51 (1987) 587.
32 M. Karplus and J.A. McCammon, FEBS Lett. 131 (1981) 34.
33 K. Gekko and Y. Hasegawa, Biochemistry 25 (1986) 6563.
34 K. Gekko and H. Noguchi, J. Phys. Chem. 83 (1979) 2706.